International Journal of Mathematical, Engineering and Management Sciences
Vol. 8, No. 2, 194-212, 2023
https://doi.org/10.33889/IJMEMS.2023.8.2.012

Wireless Sensor Network Based Real-Time Pedestrian Detection and Classification for Intelligent Transportation System

Saureng Kumar
Electronics & Computer Discipline,
Indian Institute of Technology Roorkee, Roorkee, Uttarakhand, India.
Corresponding author: skumar@pp.iitr.ac.in

S. C. Sharma
Electronics & Computer Discipline,
Indian Institute of Technology Roorkee, Roorkee, Uttarakhand, India.
E-mail: scs60fpt@iitr.ac.in

Ram Kumar
Department of Systemics, School of Computer Science,
University of Petroleum and Energy Studies, Dehradun, Uttarakhand, India.
E-mail: ram.kumar@ddn.upes.ac.in

(Received on August 23, 2022; Accepted on January 19, 2023)

Abstract
Pedestrian safety has become a critical consideration in developing society especially road traffic, an intelligent transportation need of the hour is the solution left. India tops the world with 11% of global road accidents. With this data, we have moved in the direction of computer vision applications for efficient and accurate pedestrian detection for intelligent transportation systems (ITS). The important application of this research is robot development, traffic management and control, unmanned vehicle driving (UVD), intelligent monitoring and surveillance system, and automatic pedestrian detection system. Much research has focused on pedestrian detection, but sustainable solution-driven research must still be required to overcome road accidents. We have proposed a wireless sensor network-based pedestrian detection system that classifies the real-time set of pedestrian activity and samples the reciprocally received signal strength (RSS) from the sensor node. We applied a histogram of oriented gradient (HOG) descriptor algorithm K-nearest neighbor, decision tree and linear support vector machine to measure the performance and prediction of the target. Also, these algorithms have performed a comparative analysis under different aspects. The linear support vector machine algorithm was trained with 481 samples. The performance achieves the accuracy of 98.90%and has accomplished superior results with a maximum precision of 0.99, recall of 0.98, and F-score of 0.95 with 2% error rate. The model's prediction indicates that it can be used in the intelligent transportation system. Finally, the limitation and the challenges discussed to provide an outlook for future research direction to perform effective pedestrian detection.

Keywords- Pedestrian detection, Intelligent transportation system, Unmanned vehicle driving, Machine learning, Computer vision.

Abbreviations

ADAS	: Advanced Driver Assistance System
AEBS	: Automatic Emergency Braking system
AGC	: Adaptive Gamma Correction
CNN	: Convolution Network
DACCNN	: Deep active contour convolutional neural network
EOH	: Edge Orientation Histogram
HOG	: Histogram of Oriented Gradient
ITS	: Intelligent Transportation System
LASER	: Light Amplification by Stimulated Emission of Radiation
LiDAR	: Light Detection and Ranging
MWR	: Multimeter Wave Radar
PIR	: Passive Infrared Sensor
SVM	: Support Vector Machine
UVD	: Unmanned Vehicle Driving

1. Introduction

Pedestrian safety has been the long-standing prime importance for the rapid development of intelligent transportation systems. Pedestrian detection is a highly critical and challenging task for target detection of road safety. Road safety is considerable for most important for human life. As India has the second-largest network globally. A large number of fatal accidents, disabilities, injuries, and death have been reported in the last five years. Developing countries like India, Germany and China (Li et al., 2015) deal with the latest computer vision application in pedestrian safety. However, the problem worsens in India with an alarmingly increasing a large number of pedestrian deaths, including young, adult, aged, impaired runner pedestrians, and pedestrians with guide dogs due to road accidents. According to the ministry of road transport and highway, approximately 42 casualties and the loss of fifteen lives every hour occurs in India. Pedestrian deaths in India have increased by 69% from 2015 to 2020 as shown in Figure 1. Generally, these accidents occur due to not following the road Norms and traffic norms during walking, running, and trying to cross the road during traffic. As a result, there were 23483 pedestrians were killed on the road accident in the year 2020. The number of road fatalities marks a decline of approximately 2724 pedestrian deaths recorded in Germany in 2020. China recorded 62736 fatalities in road traffic at the end of 2019. From the road safety point of view, pedestrian detection is the solution that attracts researcher's attention towards pedestrian safety. Still, there is a need to find the optimal solution to minimize this accident. With this motivation, we have proposed an intelligent transportation system based on HOG and SVM that acquires both optimal efficiency and high accuracy.

Histogram of orient gradient (HOG) is an adequate feature descriptor algorithm similar to edge orientation histogram (EOH) (Li et al., 2015) that counts occurrences of gradient orientation mainly utilized in detection and classification. In recent past years, continuous improvement in computing capability has been done. More recently, a new generation of emerging solutions exploits the features of pertinent channel parameters, including the received signal strength (RSS) of beacon packets (Palumbo et al., 2016). Earlier the research focused on efficient pedestrian detection but the existing major challenges include classification of the pedestrian, a low-level visual image descriptor are unreliable due to camera views, poses, occlusion, crowd density. Therefore, to resolve these challenges, this research work proposes an intelligent transportation system through the wireless sensor network. Specifically, we used an accelerometer and PIR sensor mounted on the vehicle's top. The received signal strength from the sensor can be used for image extraction by the HOG. The received dataset can be further pre-processed and applied a linear support vector machine algorithm for training and testing to perform efficient and accurate pedestrian detection. Also, the system counts the number of pedestrians that can help pinpoint the area for pedestrian safety.

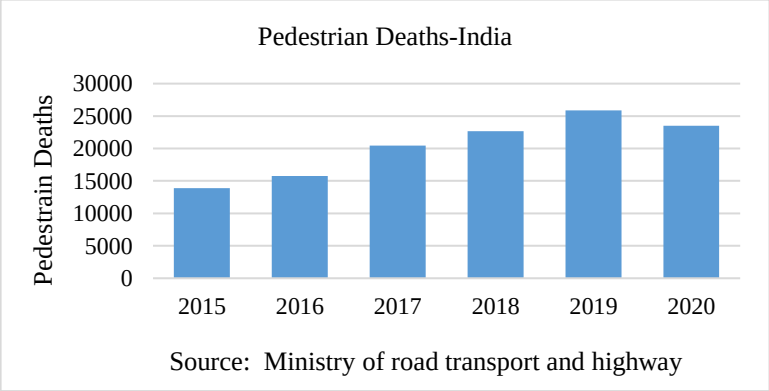

Figure 1. Pedestrian death over the past six years.

The main contributions of this work are as follows:

- Proposed a real-time pedestrian detection algorithm for the intelligent transportation system.
- The comparative analysis of publicly available benchmark datasets of pedestrians and measure the performance with ML algorithms.
- Discussed the pedestrian safety, pedestrian death, challenges of pedestrian detection and image processing of the object captured by an intelligent transportation system.
- Performed pedestrian classification based on the general concept, simulated the proposed model, and described the proposed improvements.

The remainder of the paper is organized as follows. The next section presents an overview of the various literature review and discusses the different continuing research in the subsequent section. Furthermore, we proposed an intelligent transportation system in a broader area that defines our research work and the scope of the study. Then we briefly discuss the different machine learning algorithms used in this work. In the penultimate section, we summarized the performance measure of the algorithms and the final result and discussion, which concludes in this paper.

2. Literature Review

Pedestrian detection is a unique computer vision technique in which a software system can identify, recognize, locate, and detect all known objects from a given image or video. The unique attribute of object localization is the object category (person, vehicle, dog, etc.) and the location-orientation ie; the origin of coordinates in the given image. The location is pointed to bounding box coordinates around the object to make the model's accurate performance. Since, fatal pedestrian crashes are increasing and it is significant for pedestrian safety, an innovative solution for real-time road safety using sensors for pedestrian detection. Various sensors such as Light Detection and Ranging (LiDAR) sensors, Millimeter-Wave Radar (MWR) sensors, Ultrasonic sensor, piezoelectric sensor, LASER sensor and camera is used to detect a pedestrian. The author, Nauth et al. (2019) proposed an ultrasonic backscattered signal to differentiate the vehicle or object. However, some of the studies suggested that the accuracy of the backscattered signal depends on signal frequency (Jin et al., 2015). Therefore, a PIR sensor has been presented for this research.

Several studies have been conducted for pedestrian safety, like the pedestrian-to-vehicle wireless communication (Sugimoto et al., 2008) system that helps alert pedestrians and vehicles with collisions. Vehicle technology-based pedestrian system detects pedestrians and avoids collisions through Advanced Driver Assistance Systems (ADAS) (Neuhuber et al., 2022) and Automatic Emergency Braking system (AEBS) (Rajendar et al., 2022). This system became more popular, but maintaining the speed limit is the major drawback. To maintain continuous tracking and positioning, optimal camera-based image processing provides better accuracy. The author Xu et al. (2021) claimed the 90% accuracy with the highest success rate and no pedestrian missing. However, a low-cost terminal infrared sensor can achieve a good performance on pedestrian detection. Recently a number of research proposed for infrared sensor based pedestrian detection (Zhang et al., 2022) but the disadvantage of this research it cannot perform satisfactory result in case of small pedestrian. In order to achieve pedestrian small pedestrian tracking an Infrastructure-based LiDAR sensors (Zhao et al., 2019) is used to accurately detect and track at intersection. On the other hand, LASER based detecting system has become more popular that allow target tracking in wide open area. Built-in sensor-based system gathers the surrounding information (e.g., speed, accelerations, component visual integrity, etc.) still there are various challenges to acquiring efficient and accurate pedestrian detection because pedestrian images undergo low-level visual descriptors, variation in intra-class, non-constraint illumination, occlusions, different scale, illumination, variable appearance clothing, and complex background is unreliable due to mismatched posed or camera viewpoint.More of the studies have focused on deep learning algorithms, convolution networks(CNN) (Szarvas et al., 2005), Deep active

contour convolutional neural network (DACCNN) (Raj et al., 2022) region convolution networks (RCNN) (Dong and Wang, 2016), Faster Region-based Convolutional Neural networks (F-RCNN) (Zhang et al., 2016) we have added an extra effort to check the neighborhood pixel of every single pixel through the sliding window technique. Our aim to maintain the speed limit without detoriating the image pixel. To check the darker pixel with respect to the neighborhood pixel then it shows an arrow of the image getting darker for each pixel. Therefore, this paper uses a HOG technique and the SVM algorithm to classify the pedestrian in the first stage. It performs quick classification with an image pixel enhancement.

3. Object Detection and Processing Technique

Object detection technique aims to detect quickly and accurately identify the object. The object, for instance, is like people, vehicles, faces, pedestrians, etc in an image or video. It is a challenging task when the object is under poor illumination (direct sunlight, insufficient light), suddenly changes the environment, and variation in the targeted object (Srinivas et al., 2022).
A good object detection model performs well:

- When the detected images cover at least 60% of the Image's area.
- When the detected images have clear boundaries.
- Detected images should be non-overlapping.
- Object localization should be 15 frames per second.

However, it depends on computer vision techniques in the other scenario.

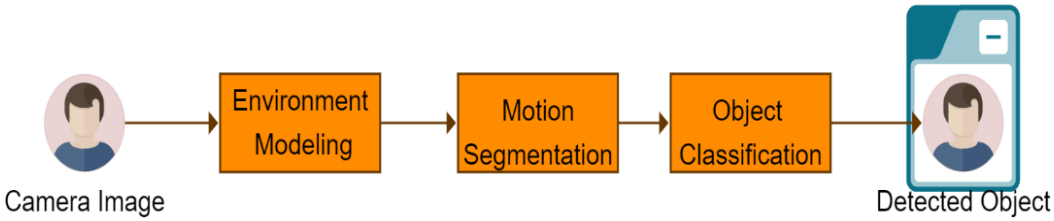

Figure 2. Schematic representation of object processing.

Figure 2 shows the steps of object processing. Firstly, an image can be acquired by any camera to create a background model. Background modeling differs from camera to camera then an environment model is constructed to make a patching-up phenomenon to acquire a holistic background image. Whenever, the images were taken in motion then motion segmentation detects the region of the moving object. Other activities like tracking and activity recognition occurred by the object classification method. Afterward, an object is detected.

4. The Proposed Pedestrian Detection System

We have proposed an efficient and accurate intelligent transportation system. The system is equipped with a wireless sensor system deployed on the top of the vehicle to achieve the objective. Despite of vast research in this area there are still significant challenges. The existing research focused a unique technique and the algorithm for the pedestrian detection. We have considered two-step solutions. Firstly, wireless sensor-based detection (accelerometer sensor, human motion sensor) that detects pedestrians within the detection range based on infrared radiation signal. For example, a PIR sensor is placed on the vehicle's top to detect the pedestrian. Secondly, visual descriptor.

We have applied HOG and Linear SVM algorithm to perform the pedestrian detection. The proposed algorithm processed in two steps. Firstly, it captures the pedestrian images, draw the rectangular frame to each pedestrian, count the pedestrian and post process the output ie; removing the overlapped boxes afterward we have applied a non-maxima suppression to suppress the boundary wall that overlaps with the significant threshold afterward gradient calculation, cell histogram generation, and block histogram normalization subsequently. The final descriptor buffer is used in the linear SVM algorithm. Secondly, we have classified the pedestrian based on received signal strength from the sensors node and the input dataset is further used for the training purpose, data preprocessing and applied the machine learning (ML) algorithm to measure the performance of the different algorithm.

Figure 3. Intelligent transportation with the pedestrian detection system.

The Intelligent transportation system with the pedestrian detection system is carried out through the vehicle's top platform, as shown in Figure 3. which is capable of classifying the pedestrian as well as automatic pedestrian detection based on the machine learning algorithm. The system is equipped with a camera and PIR sensor on the top. The goal of the sensor is to sense the motion of the pedestrian, and the camera takes the real-time images, which will be classified and processed.The system performs the two-stage analysis. real-time detection has been performed in the first stage and classification training and performance measures to be completed in the next stage.

5. Pedestrian Detection Algorithm

Pedestrian detection is an essential task that requires expert design in theoretical and practical applications. Most of the research has been conducted for the object detection algorithm like YOLO (Han et al., 2021), SSD (Li et al., 2020), and CNN (Sha and Boukerche, 2022) to accurately detect the object but still pedestrian detection is an open challenge due to background clutter and variable size in the person's appearance. Typically, the cube dimension of $100 \times 100 \times 200$ cm (for a human being's image size) is considered for the detection.

The first step is to evaluate the proposed detection algorithm.

(i) Select the object bounding box with reduced number of image points to make less computational time.
(ii) Generate a standard plane with XY, YZ and ZX axonometric projection of the image point inside the boundary box.
(iii) Create a binary image for every projection and pre-process them to create the binary seed images.
(iv) Feature extraction of every axonometric projection and Sensor node raw data to help the classification and detection.
(v) Send the feature vector to the ML algorithm for accurate prediction of the pedestrian.

HOG feature pyramid as shown in Figure 5. By using the cv2. rectangle function we draw a bounding box around detected objects. The boundary box selection is the first step of the algorithm. The algorithm is used to reduce the image points and analyze the Image captured by the sensor node.

In the second step, axonometric projection of image point is calculated through the min- max normalization formula. This technique scales the data in the range [0, 1]. The function is as follows:

$$X_{norm}^{(n)} = \frac{x^{(n)} - \min\,(x^{(n)})}{\max(x^{(n)}) - min(x^{(n)})}$$
$$Y_{norm}^{(n)} = \frac{y^{(n)} - \min\,(y^{(n)})}{\max(y^{(n)}) - min(y^{(n)})}$$
$$Z_{norm}^{(n)} = \frac{z^{(n)} - \min\,(z^{(n)})}{\max(z^{(n)}) - min(z^{(n)})}$$

Here *n* represents the number of samples and $\max\left(x^{(n)}\right)$and $\min\left(x^{(n)}\right)$are the maximum and the minimum values of the feature, respectively.

$x^{(n)}$={ $x_1, x_2, \ldots\ldots\ldots x_{ns}$},$y^{(n)}$={ $y_1, y_2, \ldots\ldots\ldots y_{ns}$},$z^{(n)}$={ $z_1, z_2, \ldots\ldots\ldots z_{ns}$} are the set of Cartesian coordinates of the image points in the sample space where ns represent the number of image points in the sample. Figure 9 shows the axonometric normalization projection of the pedestrian samples.

In the third step, we generate the binary images for every projection after min-max normalization by setting min: 0 (black) for the background and max: 1 (white) for the cloud points. Since cloud points are preprocessed and create a binary seed from a cubic region $100 \times 100 \times 200$ cm, the real cloud points are analyzed by applying several algorithms to filter the noise, outlier, and smooth object based on the feature algorithm. For this purpose, we applied a filter and morphological operation, firstly removing the noise and outlier and then smoothing the edge of the images. If the image size is big, then the algorithm is used to process into a compact size. If the Image is small, then the algorithm is usually challenging to determine.

In the fourth step, the n-dimensional vector transforms arbitrary data or images into a numerical feature representing an object (Toews and Arbel, 2003). The feature extraction and transformation, such as FFT (Kanwal et al., 2019), Wavelet transform (Tong et al., 2004) ,Gabor filter (Hoang, 2020), Dispersive Phase Stretch Transform (Asghari and Jalali, 2015) are commonly used to extract useful information. In other cases, geometric-based feature extraction and classifiers are used to find geometric features and effectively classify the Image accordingly.

To classify the pedestrian from the multiple pedestrian image, we calculate the channel binary image I. The pixel intensity by a point (x, y) where x is the reference point to the x-axis and y is the reference point to the y-axis. Hence $I(x, y) = 0\ or\ 1$

The image moment can be computed as shown in Equation (1)

$$M = \sum_x \sum_y I(x, y) \tag{1}$$

The pixel intensity has been calculated based on their intensity by a point, not based on the location. Sometimes taken Image has slightly rotated. In that case, the image moment will be the same with the different conditions. Hence, a complex moment can be computed as

$$M_{ij} = \sum_x \sum_y x^i\, y^j I(x, y) \tag{2}$$

Here i = (0,1,2,3….) and j=(0,1,2,3…..) The binary image moment contains pixels as well as the location of the Image. The centroid C can be calculated using the following formula.

$$x' = \frac{M_{10}}{M_{00}} \quad (3)$$

$$y' = \frac{M_{01}}{M_{00}} \quad (4)$$

The translation invariant, shape, and moment are computed as shown in Equation (5)

$$\mu_{ij} = \sum_x \sum_y (x - x')^i (y - y')^j I(x, y) \quad (5)$$

If the shape is the same, the moment will be the same, and then the normalized central moment is computed as

$$\eta_{ij} = \frac{\mu_{i,j}}{\mu_{00}^{\frac{(i+j)}{2+1}}} \quad (6)$$

The Hu-moment is calculated by using the central moment and invariant to image transformation from Equations (3), (4) and (5).

$$H_1 = \eta_{20} + \eta_{02} \quad (7)$$

$$H_2 = (\eta_{20} - \eta_{02})^2 + 4\eta_{11}^2 \quad (8)$$

$$H_3 = (\eta_{30} - 3\eta_{12})^2 + (3\eta_{12} - \eta_{03})^2 \quad (9)$$

$$H_4 = (\eta_{30} + \eta_{12})^2 + (\eta_{12} + \eta_{03})^2 \quad (10)$$

$$H_5 = (\eta_{30} - 3\eta_{12})(\eta_{30} + \eta_{12})[(\eta_{30} + \eta_{12})^2 - 3(\eta_{21} + \eta_{03})^2] + (3\eta_{21} - \eta_{03})(\eta_{21} + \eta_{03})[3(\eta_{30} + \eta_{12})^2 - (\eta_{21} + \eta_{03})^2] \quad (11)$$

$$H_6 = (\eta_{20} - \eta_{02})[(\eta_{30} + \eta_{12})^2 - (\eta_{21} + \eta_{03})^2 + 4\eta_{11}(\eta_{30} + \eta_{12})(\eta_{21} + \eta_{03}) \quad (12)$$

$$H_7 = (3\eta_{21} - \eta_{03}(\eta_{30} + \eta_{12})[(\eta_{30} + \eta_{12})^2 - 3(\eta_{21} + \eta_{03})^2] - (\eta_{30} - 3\eta_{12})(\eta_{21} + \eta_{03})[3(\eta_{30} - 3\eta_{12})^2 - (\eta_{21} - \eta_{03})^2] \quad (13)$$

The invariant moment $H_1, H_2, H_3 \ldots\ldots\ldots\ldots H_7$ being unchanged whenever image scaling, translation, and rotation take place. Figure 4. Shows the invariant moment with a resolution of 60×60 to 330×330. A fluctuation rapidly decreases with an increase in the spatial image resolution. When we consider the 60×60 resolution, the fluctuation shifted to 1921.1%, and when we consider the 330×330resolution, the fluctuations turned to 1.7%.

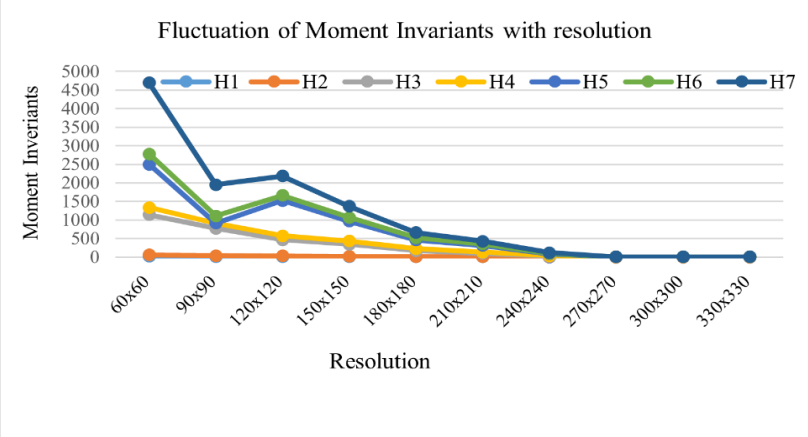

Figure 4. Fluctuation of moment invariants with different resolution.

6. Framework of the Proposed Pedestrian Detection System

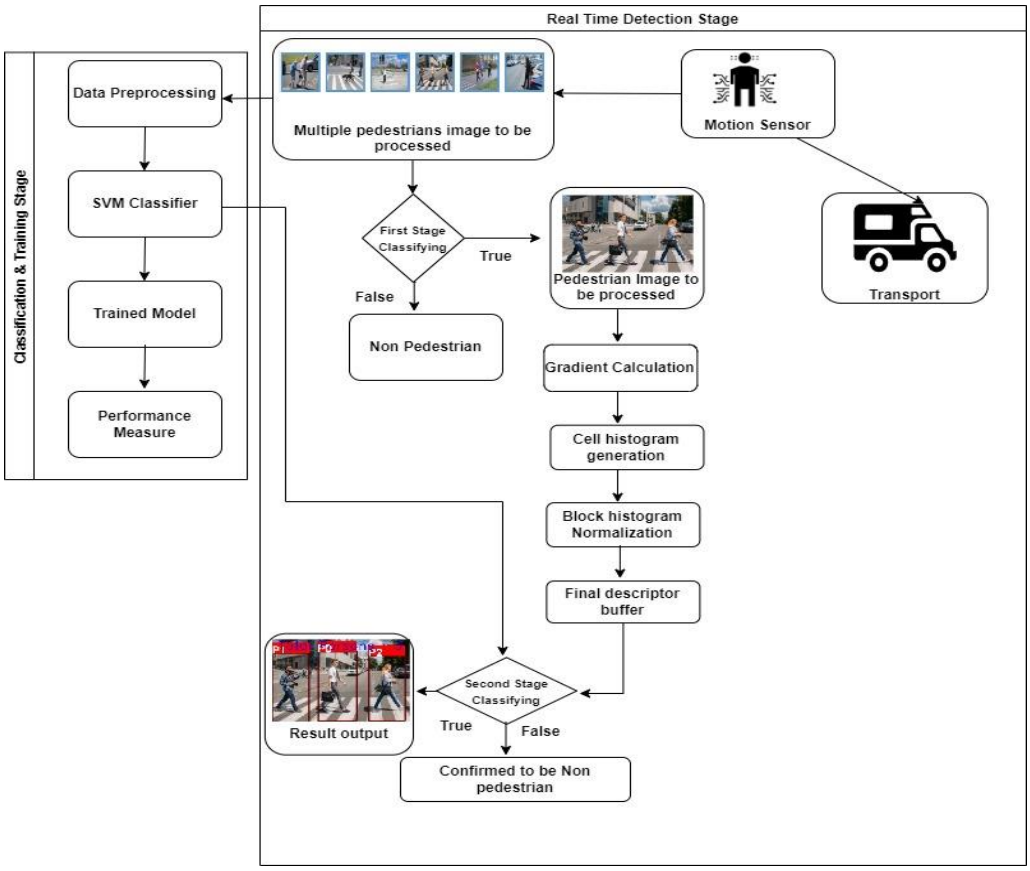

Figure 5. Framework of the proposed pedestrian detection system.

6.1 First Stage: Real-Time Detection Method

A framework of the proposed system is shown in Figure 5. In the first stage, the PIR sensor senses the pedestrian's motion, and then the camera takes the real time image. The proposed system detects and counts multiple pedestrians by using the sensor network. The sensor node senses the data and stores the data in the local storage. These data sets are preprocessed and transform the data into an understandable patch image of an image. Any size of an image is calculated on 64×128 patches of an image with a fixed aspect ratio of 1:2 for example, the Image can be $64 \times 128, 100 \times 200$, $720 \times 1440, 1080 \times 2160$. In the case of a large image with a size of 1080×2160 as shown in Figure 6. We have selected a size of 100×200 for the calculation HOG feature descriptor. The calculations proceed with four steps. In the first step, the patched Image is cropped into the size of 64×128. In this step, an adaptive gamma correction (AGC) can also perform for contrast enhancement (Rahman et al., 2016) but the minor performance improvement in the Image so we neglected this step because of different illumination conditions. This can be easily achieved by convolutional neural networks (CNN) (Chen et al., 2021). In the second step, Image is divided into 8×8 cell which contain $8 \times 8 \times 3$ pixel values, two gradient of pitch (magnitude as well as direction) per pixel a total 128 numbers to store an array of 9-bin histogram that represent less sensitive to noise. In the third step, an image enhancement technique is applied for making the Image darker by dividing pixel value by 2, and the gradient magnitude changed to half.

Therefore, the histogram values will change by half. In the fourth step, a descriptor-based independent lighting variation has been introduced for pedestrian detection in ideal and noise conditions, generally, noise image has low histogram dimensionality. To increase the illumination a color descriptor proposed for illumination variation (van de Sande et al., 2008).

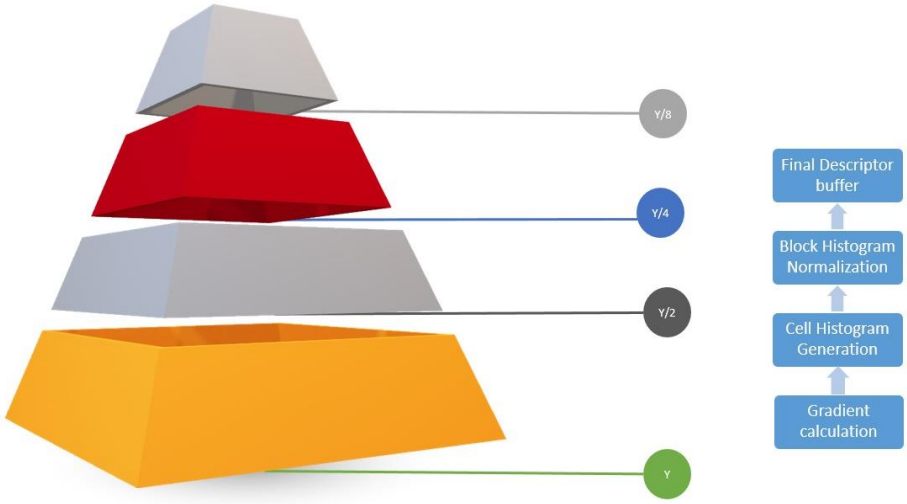

Figure 6. Histogram of the oriented gradients feature pyramid.

6.2 HOG: Feature Extraction Method

In this paper, we use the RSS sample, and the patched image size is $\mathbf{64 \times 128}$ with a fixed aspect ratio of 1:2, a person is well detected. The HOG feature calculation in the following step.

Step 1: Gradient Calculation

Calculate the Image's magnitude C(x,y) and orientation G(x,y).

$$\boldsymbol{C}(x,y) = \sqrt{f_x(x,y)^2 + f_y(x,y)^2} \tag{14}$$

$$G(x,y) = tan^{-1}\frac{f_x(x,y)}{f_y(x,y)} \tag{15}$$

Now, we calculate $f_x(x,y)\ and\ f_y(x,y)$ by using the above Equation (14) and (15)

$$f_x(x,y) = I(x+1,y) - I(x-1,y) \tag{16}$$

$$f_y(x,y) = I(x,y+1) - I(x,y-1) \tag{17}$$

Step 2: Cell Histogram Generation

To generate the cell histogram, firstly, we decrease the amount of information that the oriented gradient by dividing the window into an adjacent and non-overlapping section of the image. Here, the orientation of the histogram is 8×8 pixels with 9 bins per cell size.

Step 3: Block Histogram Normalization

Perform normalization of the histogram of data within the region using an overlapping block (16×16). ie; equal to (2×2) cell size. The cell histogram (2×2) is normalized as the final HOG feature.

Step 4: Final Descriptor Buffer
The final descriptor buffer extract feature from the image data. Here the block (cell size 4) would be buffered. Then we used SVM algorithm classifier to distinguish the pedestrian. However, the HOG and the SVM perform well in the detection and it take much time to process because of the gradient calculation.

6.3 Second Stage: Classification and Training
The classification and training are divided into following subsections.

6.3.1 Data Preprocessing
Data preprocessing is the process of transforming the raw data into relevant data for machine learning models. A raw data generally contains some missing values as a consequence of data failure or data corruption. In order to minimize this, a data preprocessing is required. The preprocessing deals with the missing value replacement. Generally, the missing value is replaced by its mean or median. This process is also known as data cleaning. The raw data will be relevant for ML model through the data cleaning process. Then after the pre-processed data was fed into the ML. This will increase the accuracy and efficiency of the model.

6.3.2 SVM Classifier
In recent years, SVM has gained importance in machine learning and has a significant research interest in this field due to its flexible application in the classification problem. The SVM classifier predicts and classifies the one-class and binary problems. The key feature is to learn through the data set and has the ability to train the model. It builds the best hyperplane in an infinite dimension plane.

6.3.3 Model Training
We collect the RSS data from the motion sensor node in the second stage. These data are preprocessed to make them suitable for the machine learning algorithm, and then we apply the support vector machine (SVM) algorithm based on the received data. SVM is used to predict and classify the one-class and binary problems and build the best hyperplane in an infinite dimension plane. The trained dataset ($\boldsymbol{T_d}$) for the binary classification is as

$$\boldsymbol{T_d} = \{(\boldsymbol{x_1}, \boldsymbol{y_1}), (\boldsymbol{x_2}, \boldsymbol{y_2}), (\boldsymbol{x_3}, \boldsymbol{y_3}), (\boldsymbol{x_n}, \boldsymbol{y_n})\}, \boldsymbol{y_i} \in \{-\mathbf{1}, \mathbf{1}\}.$$

$\boldsymbol{x_i} \in \boldsymbol{R^d}$ where $\boldsymbol{x_i}$ is the equivalent data point, $\boldsymbol{y_i}$ is the design label and n indicates the number of feature components in the trained dataset. Figure 7 shows the SVM optimal hyperplane. We aim to maximize the soft margin. The standard formulations for soft margin are as below

Minimize $\left\{\frac{\mathbf{1}}{\mathbf{2}}\boldsymbol{\beta}\acute{\boldsymbol{\beta}} + \boldsymbol{C}\sum_{\boldsymbol{i=1}}^{\boldsymbol{n}} \boldsymbol{\xi_i}\right\}, \boldsymbol{\xi_i} \geq \mathbf{0}$ (18)

Such that

$\boldsymbol{y_i}\left(\boldsymbol{\beta^T x_i} + \boldsymbol{b}\right) \geq \mathbf{1} - \boldsymbol{\xi_i}$ where, i=1, 2, n (19)

Here, C is the penalty parameter, $\boldsymbol{\xi}$ is the positive slack variable $\boldsymbol{\beta}$ is the normal vector, and b is the scalar quantity. C keeps the allowable value decreased by the Lagrangian multiplier $\boldsymbol{\alpha_i}$ that could attend Karush-Kuhn-trucker state where optimally $\boldsymbol{\alpha_i} >$, 0 then the $\boldsymbol{x_i}$ Equivalent data called support vector (SV) and SVM tries to make decision boundary with optimal hyperplane variable w and b in the succeeding formula.

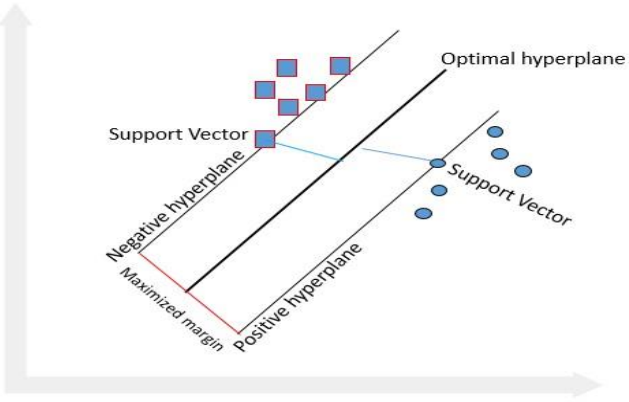

Figure 7. SVM optimal hyperplane.

$$\boldsymbol{f(x) = sgn\left(\sum_{i=1}^{n} \alpha_i y_i x_i^T + b\right)} \quad (20)$$

This expression leads directly by its unrestricted dual formation

$$\boldsymbol{Max_{\alpha} = \sum_{i=0}^{n} \alpha_i - \frac{1}{2}\sum_{i=1}^{n}\sum_{j=1}^{n} \alpha_i \alpha_j x_i x_j y_i y_j} \quad (21)$$

Subject to the constraints

$$\boldsymbol{\sum_{i=1}^{n} y_i \alpha \alpha_i = 0} \quad (22)$$

$$C \geq \boldsymbol{\alpha_i} \geq 0$$

$$\boldsymbol{w = \sum_{i=1}^{n} \alpha_i y_i x x_i} \quad (23)$$

$$\boldsymbol{b = \frac{1}{A_{sv}}(w x_i - y_i)}$$

where, $\boldsymbol{A_{sv}}$ is the amount of support vector. The proper feature mapping can make nonlinear to linear by using SVM on the feature space$\{\emptyset(\boldsymbol{x_i})\}$ only need$\emptyset(\boldsymbol{x_i})^{\boldsymbol{T}}\emptyset(\boldsymbol{x_j})$.

$$f(x) = \text{sgn}\left(\sum_{i=1}^{n} \alpha_i y_i k(x_{i,} x_j) + \mathbf{b}\right) \quad (24)$$

The kernel function $\boldsymbol{k(x_{i,}x_j)}= \emptyset(\boldsymbol{x_i})^{\boldsymbol{T}}\emptyset(\boldsymbol{x_j})$. A linear classifier gives us a nonlinear classifier with a polynomial of infinite power. The radial basis function (RBF) is a powerful kernel for any complex dataset provided by

$$\boldsymbol{k(x_{i,}x)} = \exp\left(-\frac{\|x_i - x\|^2}{2\sigma^2}\right) \quad (25)$$

Here $\boldsymbol{x_{i,}x}$ are vector points in the fixed dimensional space.

$$\boldsymbol{Max_{\alpha} = \sum_{i=0}^{n} \alpha_i - \frac{1}{2}\sum_{i=1}^{n}\sum_{j=1}^{n} \alpha_i \alpha_j y_i y_j} \exp\left(-\frac{\|x_i - x\|^2}{2\sigma^2}\right)$$

by using Equation (21)

$$C \geq \boldsymbol{\alpha_i} \geq 0$$

$$\boldsymbol{\sum_{i=1}^{n} \alpha_i y_i = 0} \quad (26)$$

The final set of inequalities, C≥ $\boldsymbol{\alpha_{,i}} \geq 0$ shows C keeps the allowable values of the lagrange multipliers αj in a box constraint. And the gradient equation solution b gives a set of nonzero $\boldsymbol{\alpha_i}$.Which correspond to the support vectors.

6.3.4 Performance Measure

We have performed this pedestrian detection and classification on the RSS dataset containing young pedestrian, runner pedestrian, aged pedestrian, adult pedestrian, impaired pedestrian, and pedestrian with a guide dog. our experiment performed on the 481 samples provided satisfactory results. among the 481 samples, the data size distribution of the pedestrian classification of young pedestrian, runner pedestrian, aged pedestrian, adult pedestrian, impaired pedestrian, and pedestrian with a guide dog are 61, 47, 116, 44,104 and 108 subsequently. As shown in Figure 8. in addition, 24.71% of instances fall under aged pedestrians, 9.17% fall in adult pedestrians, 9.79% in runner pedestrians, 12.21% of young pedestrians, 21.67% impaired pedestrians and 22.50% of pedestrians of with a guide dog is shown in Figure 9.

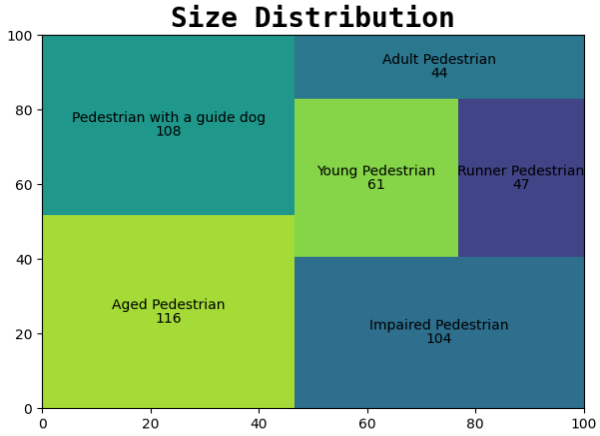

Figure 8. Dataset size distribution.

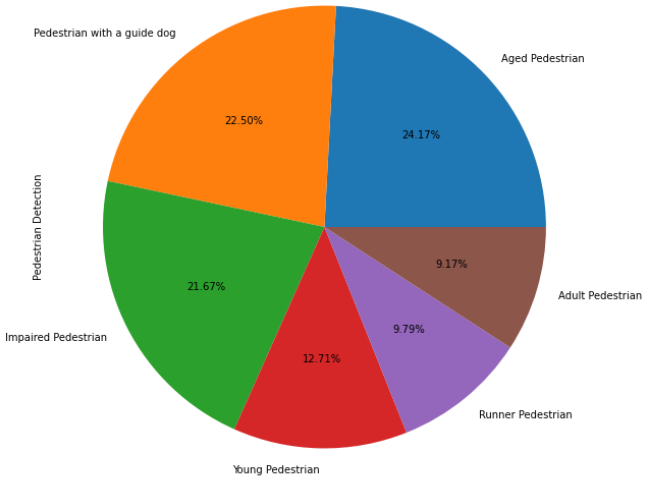

Figure 9. Percentage distribution of the dataset.

For this research, we divided the dataset, 75% for training and 25 % for testing, a heatmap of the dataset has used from RSS sensor dataset to manipulate the problem of availability (as shown in Figure 10) and then we calculated a confusion matrix for data validation. Furthermore, performance parameters are precision of 0.99, recall of 0.98 and F-score of 0.95 with a minimum 0.02 error rate. The proposed algorithm produces a relatively high pedestrian detection and an accuracy of 98.90%. also, the approach accomplished with satisfactory we have used the PIR motion sensors camera based on their RSS and camera output.

7. Result and Discussion

We have considered both pedestrian detection and pedestrian classification to perform our experiment. For pedestrian detection, we have used the HOG descriptor algorithm and the linear support vector machine algorithm for pedestrian classification. The RSS data from the PIR sensor node and the additional environmental and accelerometer sensors are available for the activity recognition settings as shown in Table 1.

Table1. Intelligent transportation learning tasks and activities involved in the different ARS setting.

S. No.	Activity recognition setting	Pedestrian classification
1	RSS from WSN	Young Pedestrian Runner Pedestrian Aged Pedestrian Adult Pedestrian Impaired Pedestrian Pedestrian with a guide dog

As per the above setting, we perform the heat map and linear discriminant analysis the simulation result a shown in Figure 10 and 11.

Heat Map is a covariance matrix with two-dimensional, graphical representation of statistical data that strengthen the relationship between variable received signal strength (var_rss) and the average signal strength(avg_rss). The heat map shown in Figure 9 provides a correlation score between -1 to 1. The X-axis denotes the positions of predicted signal strength and Y-axis denotes the real signal strength. For instance, we can see that in position (var_rss12, var_rss23) the value is 0.0087, which is close to zero hence, there is no linear trend between the source and deliver and the position (var_rss23, var_rss23) the value is 1 the correlation is more positive. However, the position (avg_rss12, var_rss23) the value is -0.018, which is closer to -1 which shows the correlation coefficient of variable received signal strength increases with the decrease of average signal strength and vice versa.

Linear Discriminant Analysis (LDA) is the most common feature extraction technique represent the decision boundary among each clustered of a class. When the input sample is large, it transforms into a reduced set of features. It Computes the mean vectors for various classes of the dataset. The simulation result of the proposed model has illustrated in Figure 11. However, the effectiveness of the algorithm was determined using the performance measure.

The performance measure of RSS dataset was calculated and compared the pedestrian detector performance. The comparative details of four detectors are shown in Table 2.

Table 2. Comparison of pedestrian detector performance trained on various datasets.

Dataset	Data Size	F1-Score	Precision	Recall
Synthetic carla	2.5K	0.76	0.8	0.72
Real waymo	2.5K	0.81	0.86	0.76
Mixed synthetic and real	5K	0.84	0.89	0.8
Received signal strength	23K	**0.98**	**0.99**	**0.98**

The author, Jabłoński et al. (2022) proposed their worked on the different dataset (Synthetic Carla, Real waymo, Mixed synthetic and real) and achieve the maximum precision 0.89. However, our algorithm outer performs with a precision of 0.99. The main advantages of our algorithms are the geometric invariant image that remain unchanged under geometric transformation. It can neglect the limb movement in case of multiple pedestrians and accurately detect the object and human features. However, our algorithm is gradient noise sensitive, take more computational time, high latitude. Other factor include unused color, shape ,texture feature.

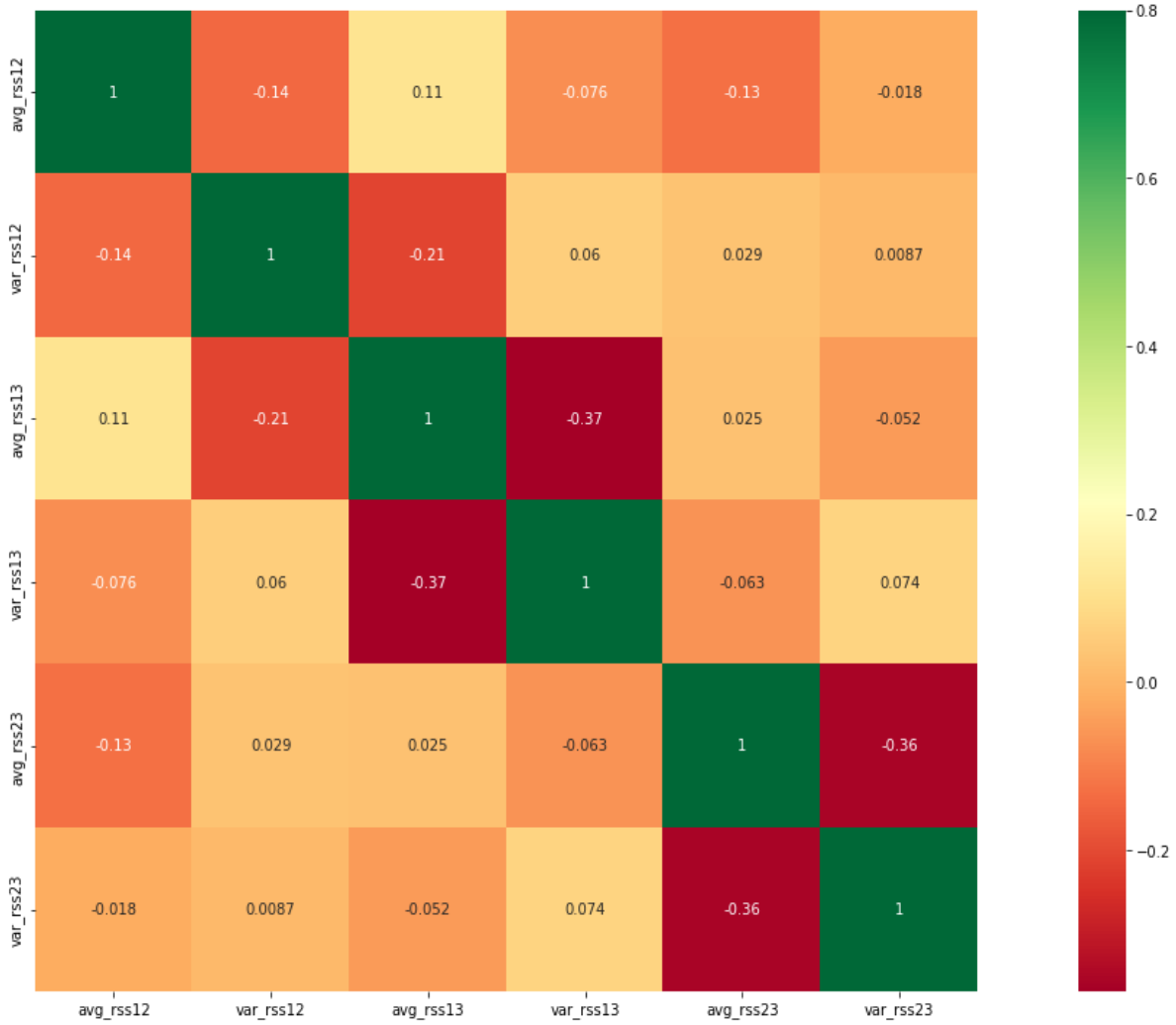

Figure 10. Heatmap of RSS sensor dataset.

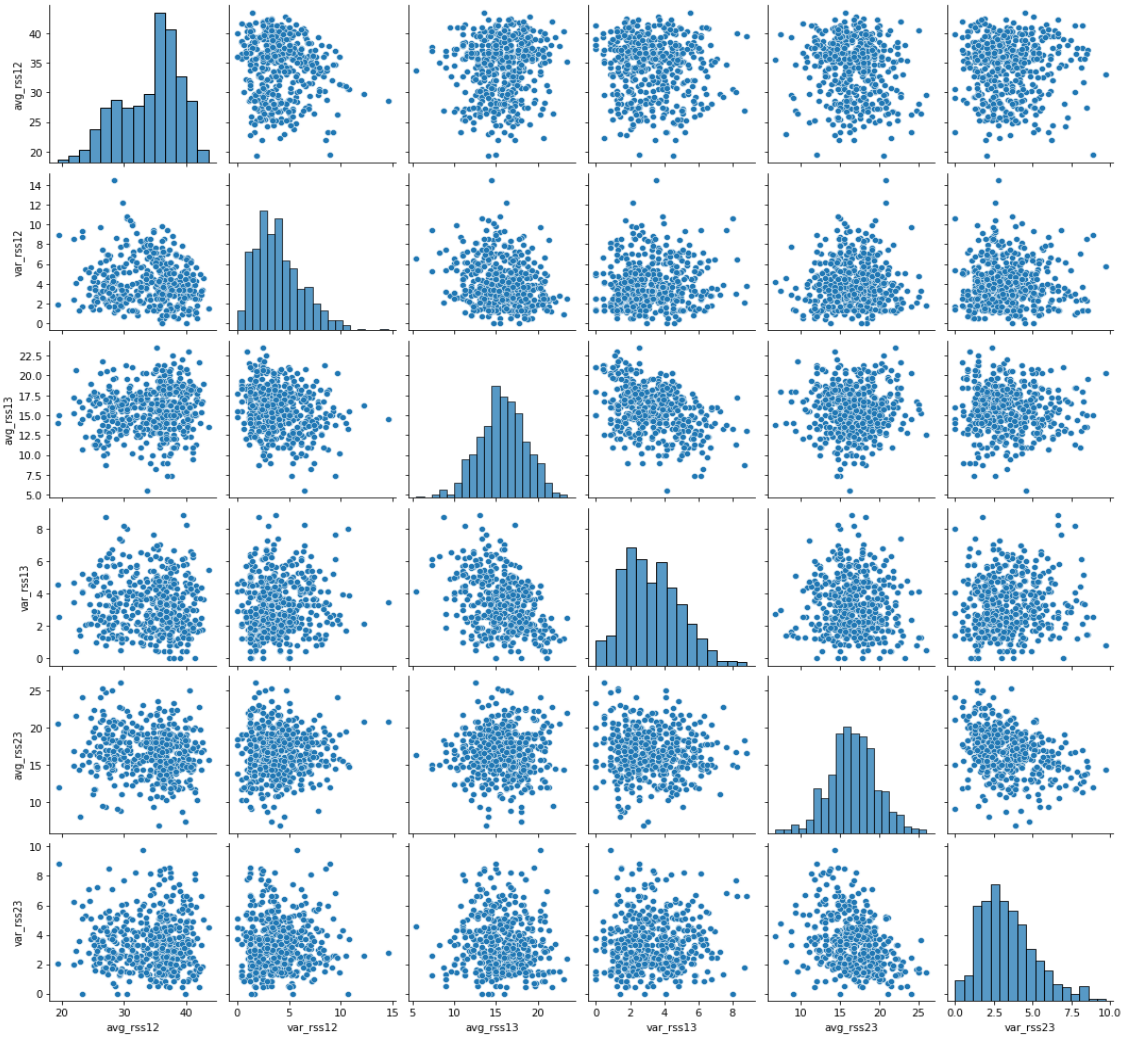

Figure 11. Illustration of linear discriminant analysis for RSS sensor dataset.

Table 3. Comparative analysis of the ML algorithms.

ML Algorithms	Performance Evaluation				
	F1-score	Precision	Error rate	Accuracy	Recall
Linear SVM	0.95	0.99	0.02	0.98	0.98
K-Nearest Neighbour	0.99	0.84	0.19	0.81	0.81
Decision Tree	0.86	0.94	0.136	0.86	0.80

This study proposed a pedestrian detection and classification technique to detect pedestrians and classify them in real-time in any environment. To execute the proposed system, we have used python programming and OpenCV 2.4.8 by HOG-SVM then, the pedestrian's Image were scaled to $\mathbf{330 \times 330}$ and the feature were extracted in 3D vector. In the classification and training stage, we trained the model and test were carried out based on RSS dataset received from the sensor node, the sensor node deployed over the vehicle. We have considered the real-time scenario in the traffic. Our proposed system achieves the precision=0.99, recall=0.98, F score=0.95 and 2% error rate with a very few false positive and false negative result obtain.

The result is shown in the Table 3. The pedestrian detection widely used in the automobile sector for improving the safety system of the vehicle. According to India union ministry road transport and highway pedestrian death gone up by 70% from 2015 to 2020. The data may further increase as per current scenario. To avoid this death, an intelligent transport system enabled by windshield camera or sensor over the vehicle must be adopted for automatic emergency braking system and intended to stop the vehicle if it detects a pedestrian in its path.

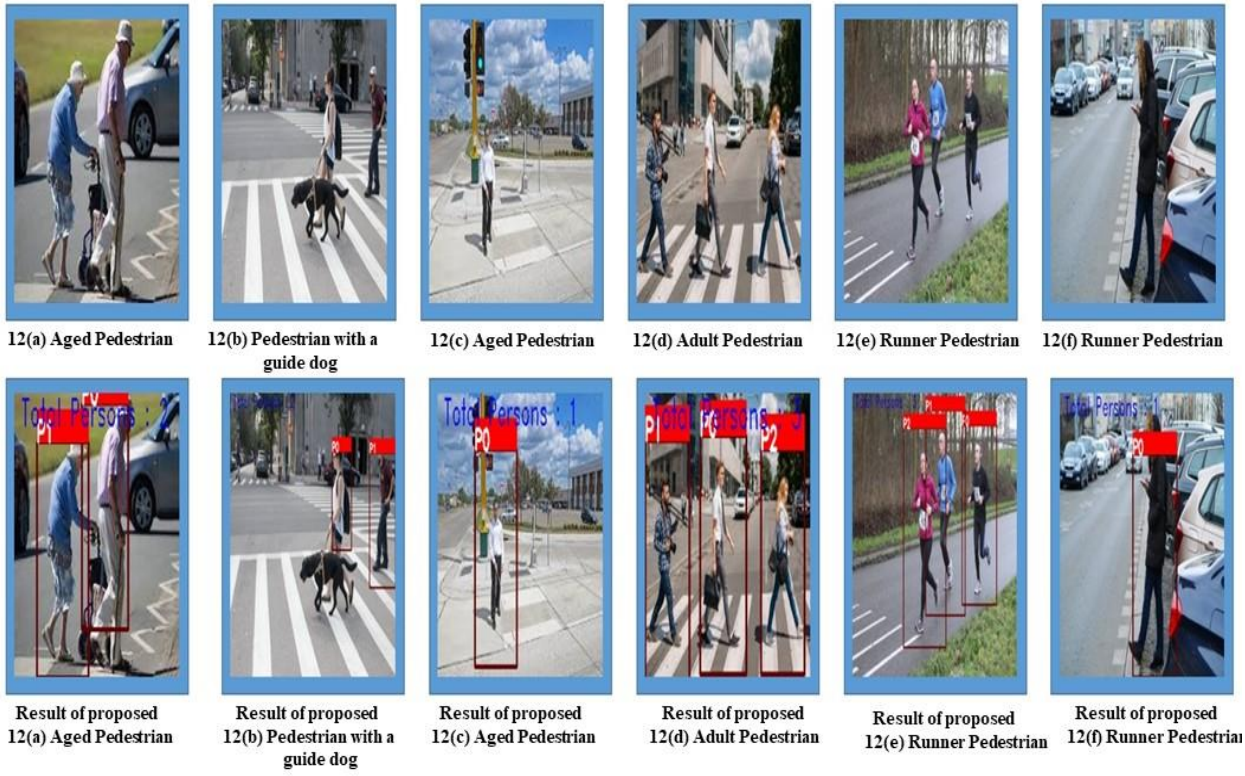

Figure 12. Example of some experiments of various pedestrians under an urban scenario.

Figure 12 shows the example of some experiments of various pedestrians under an urban scenario. The proposed result of Figure 12 (a), 12 (c), 12(d), 12(e) and 12 (f) shows the multiple detection and counting of aged pedestrian, adult and runner pedestrian. However, all pedestrian has been correctly detected but still some false positive exist in the 12(b). The pedestrian with a guide dog and another pedestrian without a guide dog that can also detected and likely to classified as pedestrian with a guide dog besides this overlapping, occluding of pedestrians causes a false alarm.

8. Conclusions

In this work, we have proposed an innovative solution for intelligent transportation systems that improve the safety system. In general, it is distinguished a little more complicated multiple pedestrians and other objects in pedestrian safety. To ensure surveillance, traffic safety from the moving pedestrians safety such as Young Pedestrian, Runner Pedestrian, Aged Pedestrian, Adult Pedestrian, Impaired Pedestrian, and Pedestrian with a guide dog. We have proposed a real time intelligent transportation system. In the first stage, we have generated multiple pedestrians using the PIR sensor-based camera and classify the non-pedestrian through the SVM based classifier. This will reduce the detection time. At the second stage,

multiple pedestrians were scaled to 330×300 and their feature were extracted by the HOG feature extraction method. The pedestrian class segmented in order to filter out the false detections. The performance achieves the accuracy of 98.90% and has accomplished superior results with a maximum precision of 0.99, recall of 0.98, and F-score of 0.95 with 2% error rate. The developed solution has used the image processing method for pedestrian detection system that proves the model's effectiveness. Through this work, an advanced safety systems for the intelligent transportation can be developed to save lives. However, the model can also be used in the video dataset for future research to perform the traffic safety also it may be used for advanced driver-assistance system (ADAS) features like automatic emergency braking system (AEBS) through this we can reduce the fatal pedestrian crashes.

Conflict of Interest

Authors declare that there is no conflict of interest.

Acknowledgements

This research did not receive any specific grant from funding agencies in the public, commercial, or not-for-profit sectors. The authors thank the editor and anonymous reviewers for their comments that help improve the quality of this work.

References

Asghari, M.H., & Jalali, B. (2015). Edge detection in digital images using dispersive phase stretch transform. *International Journal of Biomedical Imaging*, *2015*, 1-6. https://doi.org/10.1155/2015/687819.

Chen, X., Liu, L., & Tan, X. (2021). Robust pedestrian detection based on multi-spectral image fusion and convolutional neural networks. *Electronics*, *11*(1), 1. https://doi.org/10.3390/electronics11010001.

Dong, P., & Wang, W. (2016, November). Better region proposals for pedestrian detection with R-CNN. In *2016 Visual Communications and Image Processing (VCIP)* (pp. 1-4). IEEE. Chengdu, China.

Han, X., Chang, J., & Wang, K. (2021). Real-time object detection based on YOLO-v2 for tiny vehicle object. *Procedia Computer Science*, *183*, 61-72. https://doi.org/10.1016/j.procs.2021.02.031.

Hoang, N.D. (2020). Image processing-based spall object detection using Gabor filter, texture analysis, and adaptive moment estimation (Adam) optimized logistic regression models. *Advances in Civil Engineering*, *2020*, 1-16. https://doi.org/10.1155/2020/8829715.

Jabłoński, P., Iwaniec, J., & Zabierowski, W. (2022). Comparison of pedestrian detectors for LiDAR sensor trained on custom synthetic, real and mixed datasets. *Sensors*, *22*(18), 7014. https://doi.org/10.3390/s22187014.

Jin, Bo., Vai, Mang, I. (2015). An adaptive ultrasonic backscattered signal processing technique for accurate object localization based on the instantaneous energy density level. *Journal of Medical Imaging and Health Informatics*, *5*(5), 1059-1064. https://doi.org/DOI: https://doi.org/10.1166/jmihi.2015.1493.

Kanwal, N., Girdhar, A., Kaur, L., & Bhullar, J.S. (2019, April). Detection of digital image forgery using fast fourier transform and local features. In *2019 International Conference on Automation, Computational and Technology Management (ICACTM)* (pp. 262-267). IEEE. London, UK.

Li, Y., Dong, H., Li, H., Zhang, X., Zhang, B., & Xiao, Z. (2020). Multi-block SSD based on small object detection for UAV railway scene surveillance. *Chinese Journal of Aeronautics*, *33*(6), 1747-1755. https://doi.org/10.1016/j.cja.2020.02.024.

Li, Y., Shi, X., Jin, H., & Wen, Z. (2015). Detecting lines and building intersection correspondences by computing edge oriented histogram on multi-sensor images. *Infrared Physics & Technology*, *73*, 1-7. https://doi.org/10.1016/j.infrared.2015.08.013.

Nauth, P.M., Pech, A.H., & Michalik, R. (2019, March). Research on a new smart pedestrian detection sensor for vehicles. In *2019 IEEE Sensors Applications Symposium (SAS)* (pp. 1-5). IEEE. Sophia Antipolis, France.

Neuhuber, N., Pretto, P., & Kubicek, B. (2022). Interaction strategies with advanced driver assistance systems. *Transportation Research Part F: Traffic Psychology and Behaviour*, *88*, 223-235. https://doi.org/10.1016/j.trf.2022.05.013.

Palumbo, F., Gallicchio, C., Pucci, R., & Micheli, A. (2016). Human activity recognition using multisensor data fusion based on reservoir computing. *Journal of Ambient Intelligence and Smart Environments*, *8*(2), 87-107. https://doi.org/10.3233/AIS-160372.

Rahman, S., Rahman, M.M., Al-Wadud, A.M., Al-Quaderi, G.D., & Shoyaib, M. (2016). An adaptive gamma correction for image enhancement. *EURASIP Journal on Image and Video Processing*, *2016*(1), 1-13. https://doi.org/10.1186/s13640-016-0138-1.

Raj, N., Perumal, S., Singla, S., Sharma, G.K., Qamar, S., & Chakkaravarthy, A.P. (2022). Computer aided agriculture development for crop disease detection by segmentation and classification using deep learning architectures. *Computers and Electrical Engineering*, *103*, 108357. https://doi.org/10.1016/j.compeleceng.2022.108357.

Rajendar, S., Rathinasamy, D., Pavithra, R., Kaliappan, V.K., & Gnanamurthy, S. (2022). Prediction of stopping distance for autonomous emergency braking using stereo camera pedestrian detection. *Materials Today: Proceedings*, *51*, 1224-1228. https://doi.org/10.1016/j.matpr.2021.07.211.

Sha, M., & Boukerche, A. (2022). Performance evaluation of CNN-based pedestrian detectors for autonomous vehicles. *Ad Hoc Networks*, *128*, 102784. https://doi.org/10.1016/j.adhoc.2022.102784.

Srinivas, K., Singh, L., Chavva, S.R., Dappuri, B., Chandrasekaran, S., & Qamar, S. (2022). Multi-modal cyber security based object detection by classification using deep learning and background suppression techniques. *Computers and Electrical Engineering*, *103*, 108333. https://doi.org/10.1016/j.compeleceng.2022.108333.

Sugimoto, C., Nakamura, Y., & Hashimoto, T. (2008, March). Development of pedestrian-to-vehicle communication system prototype for pedestrian safety using both wide-area and direct communication. In *22nd International Conference on Advanced Information Networking and Applications* (AINA 2008) (pp. 64-69). IEEE. Gino-wan, Japan.

Szarvas, M., Yoshizawa, A., Yamamoto, M., & Ogata, J. (2005, June). Pedestrian detection with convolutional neural networks. In *IEEE Proceedings. Intelligent Vehicles Symposium, 2005* (pp. 224-229). IEEE. Las Vegas, NV, USA.

Toews, M., & Arbel, T. (2003, October). Entropy-of-likelihood feature selection for image correspondence. In *Computer Vision, IEEE International Conference on* (Vol. 3, pp. 1041-1041). IEEE Computer Society. Nice, France.

Tong, H., Li, M., Zhang, H., & Zhang, C. (2004, June). Blur detection for digital images using wavelet transform. In *2004 IEEE International Conference on Multimedia and Expo* (ICME) (Vol. 1, pp. 17-20). IEEE. Taipei, Taiwan.

van de Sande, K.E.A., Gevers, T., & Snoek, C.G.M. (2008). Evaluation of color descriptors for object and scene recognition. *2008 IEEE Conference on Computer Vision and Pattern Recognition*, 1-8. https://doi.org/10.1109/CVPR.2008.4587658.

Xu, X., Li, X., Zhao, H., Liu, M., Xu, A., & Ma, Y. (2021). A real-time, continuous pedestrian tracking and positioning method with multiple coordinated overhead-view cameras. *Measurement*, *178*, 109386. https://doi.org/10.1016/j.measurement.2021.109386.

Zhang, J., Liu, C., Wang, B., Chen, C., He, J., Zhou, Y., & Li, J. (2022). An infrared pedestrian detection method based on segmentation and domain adaptation learning. *Computers and Electrical Engineering*, *99*, 107781. https://doi.org/10.1016/j.compeleceng.2022.107781.

Zhang, L., Lin, L., Liang, X., & He, K. (2016). Is faster R-CNN doing well for pedestrian detection? In: Leibe, B., Matas, J., Sebe, N., & Welling, M. (eds) *Computer Vision – ECCV 2016* (Vol. 9906, pp. 443-457). International Publishing. Springer. https://doi.org/10.1007/978-3-319-46475-6_28.

Zhao, J., Xu, H., Liu, H., Wu, J., Zheng, Y., & Wu, D. (2019). Detection and tracking of pedestrians and vehicles using roadside LiDAR sensors. *Transportation Research Part C: Emerging Technologies*, *100*, 68-87. https://doi.org/10.1016/j.trc.2019.01.007.